M-PM-Sym-1

SINGLE PARTICLE TRACKING OF CELL SURFACE COMPONENTS USING NANOVID MICROSCOPY. ((K. Jacobson, R. Simson, B. Yang, and G. Lee)) Dept. of Cell Biology and Anatomy, University of North Carolina at Chapel Hill, Chapel Hill, NC 27599-7090

The use of Nanovid microscopy to obtain the trajectories of mobile cell surface molecules can be regarded as a breakthrough in the study of the dynamic structure of membranes and associated macromolecules. Typically, nanometer sized gold or fluorescent particles are coated with antibodies to the molecule of interest. The particles are visualized with video-enhanced light microscopy and their sequential positions are traced with digital image processing. To introduce this session, sample applications of this new technology will be presented. Gold-lipid probes in both supported bilayers and in cell membranes exhibit simple, unconstrained diffusion. Preliminary analysis of the mobility of NCAMs expressed via gene transfer in 3T3 cells indicates that these molecules also show simple diffusion with an "immobile fraction" in agreement with photobleaching results. But single particle tracking allows the immobile fraction to be resolved into two components: one stationary and one confined to small regions. Aggrecan-hyaluronan complexes of the pericellular matrix exhibit restricted diffusion that can be interpreted as a wobbling-in-a-cone motion due to tethering to a cell membrane receptor. Supported by NIH GM 41402.

M-PM-Sym-2

SINGLE-PARTICLE TRACKING IN AN ARCHIPELAGO. ((Michael J. Saxton)) Institute of Theoretical Dynamics, University of California, Davis, California 95616, and Laboratory of Chemical Biodynamics, Lawrence Berkeley Laboratory, Berkeley, California 94720.

Single-particle tracking experiments measure trajectories of individual membrane proteins on the cell surface, providing highly detailed information on membrane dynamics. But data analysis for these experiments must take into account the statistical fluctuations that occur in individual random walks. With distressingly high probability, purely random walks show structure that suggests biologically important processes such as obstructed motion, directed motion, or trapping in bounded domains. To interpret observed trajectories correctly, one must consider not only the trajectories themselves but also the probabilities of occurrence of various trajectories. And one must use the proper control: a two-dimensional unobstructed random walk. Techniques for data analysis will be illustrated using two models of directed motion, one in which diffusion and bulk flow are superimposed, and one in which the observed particle is either freely diffusing or bound to a cytoskeletal conveyor belt moving with prescribed velocity. (Supported by NIH grant GM38133.)

M-PM-Sym-3

FRACTILE TIME TRANSPORT IN THE CELL SURFACE. ((Watt W. Webb)) Applied and Engineering Physics, Cornell University, Ithaca, NY 14853.

Our measurements of spontaneous random trajectories of individual cell surface receptor molecules have shown (Richik Ghosh and James Slattery) that the molecular mobility is restricted so that the diffusion coefficient becomes time dependent slowing with a fractional power as $D(t) = D(1)\, t^{\alpha}$ with $0 < \alpha < 1$. Usually $0.3 < \alpha < 0.9$, significantly less than the $\alpha = 1$ expected of free Brownian motion, as if the distribution of molecular dwell times were stretched from poisson to a scale free time fractal over many e-foldings in time. Summation over the distribution of trajectories of large cell surface receptor populations (Toni Feder and Ingrid Brust-Macher) accounts quantitatively for the ubiquitous and mysterious "immobile fraction" of FPR experiments as a consequence of the long time tails of molecular trajectories, even without actual immobile receptors.

Research supported by NSF(8800278) and NIH(RR04224) in the Developmental Resource for Biophysical Imaging and Opto-electronics.

M-PM-Sym-4

CONFINED LATERAL DIFFUSION OF MEMBRANE RECEPTORS AS STUDIED BY SINGLE PARTICLE TRACKING AND LASER TWEEZERS. ((Akihiro Kusumi)) Department of Pure and Applied Sciences, The University of Tokyo, Meguro-ku, Tokyo 153, Japan.

Movements of transferrin and α_2-macroglobulin receptor molecules in the plasma membrane of cultured normal rat kidney (NRK) fibroblastic cells were investigated by video-enhanced optical microscopy with 1.8 nm spatial precision and 33 ms temporal resolution by labeling the receptors with the ligand-coated nanometer-sized colloidal gold particles. For both receptor species, most of the movement trajectories are of the confined diffusion type, within domains of $\approx$ 0.25 μm^2 (500-700 nm in diagonal length). Movement within the domains is random with a diffusion coefficient $\approx 10^{-9}$ cm^2/s, which is consistent with that expected for free Brownian diffusion of proteins in the plasma membrane. The receptor molecules move from one domain to one of the adjacent domains at an average frequency of 0.034 s^{-1} (the residence time within a domain $\approx$ 29 s), indicating that the plasma membrane is compartmentalized for diffusion of membrane receptors and that long-range diffusion is the result of successive intercompartmental jumps. The macroscopic diffusion coefficients for these two receptor molecules calculated on the basis of the compartment size and the intercompartmental jump rate are $\approx 2.4 \times 10^{-11}$ cm^2/s, which is consistent with those determined by averaging the long-term movements of many particles. Partial destruction of the cytoskeleton decreased the confined diffusion mode, increased the simple diffusion mode, and induced the directed diffusion (transport) mode. These results suggest that the boundaries between compartments are made of dynamically fluctuating membrane skeletons (membrane-skeleton fence model).

M-PM-Sym-5

Single Particle Tracking (SPT) measurements of glycoprotein movements in cell migration. Michael P. Sheetz

The migration of fibroblastic cells in vitro involves a carefully orchestrated series of glycoprotein movements that involve attachment and detachment of cytoskeletal linkages. The digital tracking of particles attached to glycoproteins (SPT) on the dorsal surface has provided a number of important insights into the basic glycoprotein movements underlying cell migration. SPT measurements show that transport of particles rearward involves attachment to the cytoskeleton whereas forward movements of diffusing particles occurs. In addition, there is a preferential concentration of certain glycoproteins at curved regions of membrane. In these phenomena there is no detectable bulk flow of membrane or lipid relative to the cell outline. At the leading edge there is preferential attachment of crosslinked integrins to the cytoskeleton and such cytoskeletal attachments are lost at the rear of the cell (Schmidt et al., J. Cell Biol. in Press). Such graded attachments are essential for the cell to be able to release and migrate forward. In regard to the site of force generation for movement, we postulate that motors at the boundary of the endoplasm and ectoplasm are pulling on the cortical actin. Because the cortical actin is anchored to the external matrix more strongly at the front of the cell than at the rear, contraction by the endoplasmic structure will pull the cell forward. SPT provides the means to study rearward transport of crosslinked, forward movements of diffusing, and concentration by curvature of membrane glycoproteins.

M-PM-A1

CARDIAC Ca^{2+} RELEASE CHANNEL IS A HIGH AFFINITY RECEPTOR FOR CARDIAC GLYCOSIDES. ((L.J. Hymel, A. Whitworth, S.N. Wang and C.W. Clarkson)) Depts. of Physiology and Pharmacology, Tulane University School of Medicine, New Orleans, LA 70112.

Cardiac glycosides are classically thought to enhance myocardial contractility by blocking Na^+,K^+-ATPase with consequent elevation of cytosolic [Ca^{2+}]. Recently, alternative targets have been considered, including the sarcoplasmic reticulum (SR) Ca^{2+} release channel (CRC, ryanodine receptor). We have performed Scatchard analysis of ^{3}H-digitoxin binding to canine cardiac SR terminal cisternae (TC) vesicles and found a single high affinity binding site with B_{max} = 3.8 pmol/mg and K_d = 12.5 nM, similar to the binding of ^{3}H-ryanodine (B_{max} = 4.5 pmol/mg, K_d = 4.4 nM). Solubilization of the TC membranes with CHAPS/SBL and affinity chromatography on spermine agarose led to copurification of both digitoxin and ryanodine binding acitivities by 7-fold with retention of nM binding affinity (digitoxin, B_{max} = 26 pmol/mg, K_d = 56 nM; ryanodine, B_{max} = 33 pmol/mg, K_d = 20 nM). We have also investigated the effects of digitoxin on resting [Ca^{2+}] using single Fura-2 loaded guinea pig ventricular myocytes. Exposure to 5 μM digitoxin produced a biphasic effect: an acute transient elevation of Ca^{2+} (within seconds), whose size depended on the level of Ca^{2+} preloading of the SR, followed by a smaller but continuous increase of resting [Ca^{2+}] over many minutes. These results are consistent with a rapid activation of the CRC by digitoxin (acute response) in addition to longer term elevation of resting [Ca^{2+}] via the classical mechanism. The observed 1:1 stoichiometry and copurification of digitoxin and ryanodine binding activities suggest that the CRC is a primary molecular target of these cardiotonic drugs. Supported by grants from the American Heart Association, La. Affiliate Inc. and the Louisiana Board of Regents to L.H.

M-PM-A2

THREE-DIMENSIONAL CRYO-ELECTRON MICROSCOPY OF THE CALCIUM RELEASE CHANNEL/RYANODINE RECEPTOR (RyR) FROM SKELETAL MUSCLE. ((M. Radermacher, V. Rao, T. Wagenknecht, R. Grassucci, J. Frank, A.P. Timerman, and Sidney Fleischer)) Wadsworth Center for Laboratories and Research, N.Y. State Dept. of Health, Albany, NY 12201 and Department of Molecular Biology, Vanderbilt University, Nashville, TN 37235. (Spon. by W. Tivol).

The 3D architecture of the RyR was determined from a random conical tilt series extracted from electron micrographs of isolated detergent-solubilized channels prepared in a frozen-hydrated state. From 9 pairs of micrographs, corresponding to tilted and non-tilted specimen, images of 1,665 particles were selected that had adsorbed to the carbon support film in the 4-fold symmetric orientation. Following alignment and multivariate statistical analysis, two major classes of particles were identified that corresponded to right-side-up and upside down RyR's. Independent 3D reconstructions, determined for each of the two classes, showed only minor differences. The reconstructions exhibited reproducible details to 3.2 nm, and revealed significantly more structural information than our previously reported reconstruction from a negatively stained specimen. The height of the basal platform, present on one face of the channel and thought to contain the transmembrane domain, is greater in the new reconstruction (8 vs 4 nm). The large cytoplasmic domain shows a much more convoluted distribution of protein and solvent than was observed in negative stain, and is suggestive of a structural framework. Supported by NIH AR40615 (TW), NIH GM29169 (JF), and NIH HL32711 (SF).

M-PM-A3

LOCALIZATION OF CALMODULIN BINDING SITES ON THE SKELETAL MUSCLE RYANODINE RECEPTOR BY ELECTRON MICROSCOPY. ((T. Wagenknecht, J. Berkowitz, R. Grassucci, A.P. Timerman, and Sidney Fleischer)) Wadsworth Center for Laboratories and Research, New York State Dept. of Health, Albany, NY 12201 and Department of Molecular Biology, Vanderbilt University, Nashville, TN 37235.

Calmodulin (CaM) is a regulator of the calcium release channel (ryanodine receptor, RyR) from sarcoplasmic reticulum of skeletal and cardiac muscle. To locate the binding site of CaM on the RyR we formed CaM:RyR complexes in vitro from purified rabbit skeletal muscle RyR and wheat germ CaM. The CaM for these studies was covalently linked via the free sulfhydryl group on cys-27 to a 1.4-nm diameter gold cluster. Electron microscopy of negatively stained or frozen-hydrated complexes showed that the gold clusters bind near the corners of the square-shaped RyR. Up to 4 gold clusters could bind to a single tetrameric RyR. Precise mapping (in two dimensions) of the gold cluster locations on the images was accomplished by computerized averaging applied to micrographs of frozen-hydrated complexes. No changes in the structure of the RyR upon binding CaM were detectable at the resolution of the analysis, about 3 nm. Based on these results and our previously determined three-dimensional reconstruction of the RyR in the absence of CaM, it is apparent that the CaM-gold clusters bind near the periphery of the large cytoplasmic domain (i.e. the foot region) of the RyR. We conclude that the CaM binding site is 5-10 nm from the transmembrane channel of the RyR. Apparently long-range conformational changes are involved in the modulation of RyR activity by CaM. Supported by NIH AR40615 (TW) and NIH HL32711 (SF).

M-PM-A4

FKBP12 OPTIMIZES FUNCTION OF THE CLONED EXPRESSED CALCIUM RELEASE CHANNEL (RYANODINE RECEPTOR) ((A-M. B. Brillantes, K. Ondrias, T. Jayaraman, A. Scott, E. Kobrinsky, B. E. Ehrlich*, and A. R. Marks)) Mount Sinai School of Medicine, N.Y., N.Y. 10029 and *Univ. of CT, Farmington, 06032

Intracellular Ca release channels participate in signaling pathways controlling muscle contraction, hormone and neurotransmitter release and cell growth and differentiation. Ultrastructural, biochemical, and cloning studies have suggested that the Ca release channel/ryanodine receptor (RyR) is a homotetramer of four 565 kDa RyRs. Here we report that the function of the cloned expressed RyR is optimized after addition of recombinant FK-506 binding protein (FKBP12), a 12 kDa *cis-trans* peptidyl-prolyl isomerase that co-purifies with the native RyR. Recombinant RyR, expressed in insect cells that do not contain FKBP12, consistently exhibited single channel properties similar to those of the native RyR. However, addition of recombinant FKBP12 significantly increased the frequency of channels exhibiting the full conductance state, similar to that reported for native RyRs. The response to compounds known to modulate the channel was unchanged. Our findings support the idea that the Ca release channel is actually a complex of at least two molecules, the RyR and FKBP12, and that FKBP12 optimizes the behavior of the channel.

M-PM-A5

HIGHLY COOPERATIVE AND HYSTERESIS RESPONSE OF THE SKELETAL MUSCLE RYANODINE RECEPTOR TO CHANGES IN PROTON CONCENTRATIONS. ((Jianjie Ma and Ji-ying Zhao)) Dept. of Physiol. and Biophys., Case Western Reserve Univ., Cleveland, OH 44106.

The skeletal muscle Ca release channels reconstituted into lipid bilayers had two open states of 0.4 ms and 2.8 ms at 100 uM [Ca]$_i$ and 2 mM [ATP]$_i$ (-50 mV test potential). Multiple proton titration sites are involved in controlling the different open states of the channel, as indicated by the following: i) The channel had a biphasic response to changes in proton concentrations around pK = 7.6; ii) The activities of the channel were inhibited by acidic pHs in a highly cooperative manner (pK = 6.5, n_H = 3.7); and iii) The channel exhibited pronounced hysteresis to changes in pH (acidic titration and alkaline recovery were separated by ~ 1 pH unit). The hysteresis behavior was more prominent in the ryanodine activated channel. Ryanodine shifted the acidic titration curves to the left (pK = 4.9-5.4, depending on the level of [Ca]$_i$ and [ATP]$_i$). Two types of channel recovery were observed: partial recovery of sub-conductance states at uM [Ca], and complete recovery of full conductance state observed at nM [Ca]. Four distinct conductance states (255 pS, 200 pS, 128 pS, 65 pS) were identified in the single ryanodine activated Ca release channel. The distribution of the multiple conductance states depended on the level of [Ca], ATP and pH in the recording solution. The data suggest that the calcium release channels are formed by multimers, likely to be tetramers, of the 560 kDa ryanodine receptor. Supported by NIH and MDA.

M-PM-A6

ACTIVATION OF THE SKELETAL MUSCLE CALCIUM RELEASE CHANNEL BY A CYTOPLASMIC LOOP OF THE DIHYDROPYRIDINE RECEPTOR ((Xiangyang Lu, Le Xu and Gerhard Meissner)) Department of Biochemistry and Biophysics, University of North Carolina, Chapel Hill, NC 27599-7260. (Spon. by Jan Hermans)

Expression studies with skeletal and cardiac muscle cDNAs have suggested that the putative cytoplasmic loop region of the dihydropyridine receptor (DHPR) α1 subunit between transmembrane repeats II and III (DCL) is a major determinant of the type of excitation-contraction coupling in rescued dysgenic muscle cells. In this study, the possibility of a direct functional interaction with the sarcoplasmic reticulum Ca^{2+} release channel/ryanodine receptor has been tested by expressing the DCLs of the mammalian skeletal and cardiac muscle DHPR α1 subunit in *E. coli*. The purified peptides activated the skeletal muscle sarcoplasmic reticulum Ca^{2+} release channel by increasing channel open probability and the affinity of [^{3}H]ryanodine binding. The two peptides did not activate the cardiac muscle Ca^{2+} release channel. Other proteins also increased [^{3}H]ryanodine binding and Ca^{2+} release channel activity, but their activation mechanisms were distinguishable from DCLs. These results show that the II-III cytoplasmic loop of the skeletal and cardiac DHPR α1 subunit functionally interacts with the skeletal, but not cardiac, muscle Ca^{2+} release channel. Furthermore, our studies suggest that in addition to the DHPR, the sarcoplasmic reticulum Ca^{2+} release channel may determine the type of E-C coupling that exists in muscle.

M-PM-A7

MODELS OF SIMULTANEOUS INTERACTIONS OF THE SKELETAL MUSCLE Ca RELEASE CHANNEL WITH Ca, Mg AND ATP. ((I.Stavrovsky, J.Zhou and E.Rios)) Rush Univ., Chicago, IL 60612. (Spon. by F.Quandt)

The main results in the preceding poster (Zhou et al. 1994) are that ATP increases Po of Ca release channels by a constant factor at all $[Ca^{2+}]$ and that Mg^{2+} reduces Po without changing the optimal $[Ca^{2+}]$, while increasing cooperativity of activation. Models were tested to explain these results.

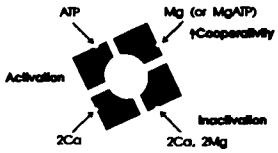

In the models, the channel opens by non-cooperative binding of one or two Ca^{2+} ions to its closed state, with high affinity but very small equilibrium constants of opening transitions. These are significantly increased by binding one ATP molecule. Inactivation at high $[Ca^{2+}]$ is explained by independent low-affinity Ca^{2+} binding site(s) accessible from all states. This scheme reproduces the observed scaling effect of ATP, with minimum shift in Ca^{2+}-dependence.

To interpret the apparent high cooperativity of Ca^{2+} activation at $[Mg^{2+}]$ as low as 50μM, we assumed the existence of a high-affinity site for Mg^{2+} or ATP-Mg, inducing a dramatic increase in cooperativity of Ca^{2+} binding, with no inhibition effect. Three mechanisms of actual inhibition by Mg^{2+} were tested. A second Mg^{2+} site, reducing the opening equilibrium constants, could not reproduce the measured sigmoidicity of Po vs $[Mg^{2+}]$. Competitive Mg^{2+} binding at Ca^{2+} activating sites yielded expected shapes of Ca^{2+} and Mg^{2+} dependencies but shifted optimal $[Ca^{2+}]$ to higher values. Cooperative binding of two Ca^{2+} and two Mg^{2+} to the same inactivating sites (diagram), reproduced best our experimental results. Supported by NIH and AHA.

M-PM-A8

VOLTAGE-DEPENDENT DESENSITIZATION OF RABBIT SKELETAL MUSCLE RYANODINE RECEPTOR: EVIDENCE FOR TWO TYPES OF Ca RELEASE CHANNELS. ((J. Ma, M.A. Albrecht and J.-y. Zhao)) Dept. of Physiol. and Biophys., Case Western Reserve Univ., Cleveland, OH 44106.

The skeletal muscle Ca release channel in isolation has properties resembling a ligand gated channel. We found that a portion of the channels exhibited a characteristic voltage-dependent inactivation: i) With a test pulse of 10 s duration to -100 mV (myoplasimc-minus-luminal SR), the channel desensitized with a time constant of 3.7 s (n=11); ii) The desensitization is highly asymmetric and voltage dependent, it was only observed at voltages more negative than -80 mV; iii) The desensitization required the channel to be in the maximally opened condition, without ATP no desensitization occurred; iv) Repetitive tests to -100 mV usually led to complete immobilization of the channel (6/9 experiments). Such closed channel could be recovered by a conditioning pulse to positive voltages. Similar phenomena were also observed in the ryanodine activated channel (1 uM conc.). The long-lived open state of the ryanodine activated channel did not require the presence of ATP to enter the desensitization state. In bilayers with multiple (2-4) channels, two different effects of ryanodine were measured: i) some channels bind ryanodine faster (< 2 min.), others bind much slower (> 20 min.); ii) the faster ryanodine-binding channels always desensitize at -100 mV, while those bind slowly do not show apparent desensitization. The data suggest there are two functionally different population of Ca release channels in the rabbit skeletal muscle.

M-PM-A9

ACTIVATION OF SARCOPLASMIC RETICULUM CALCIUM RELEASE CHANNELS BY INTRALUMINAL Ca^{2+}. **((S. E. Thedford, W. J. Lederer and H. H. Valdivia)). University of Maryland at Baltimore.**

Gating of the sarcoplasmic reticulum (SR) Ca^{2+} release channel is modulated by cytosolic substances such as Ca^{2+}, Mg^{2+}, ATP and calmodulin. In addition, regenerative type Ca^{2+} release mechanisms have been shown to depend on the Ca^{2+} content within the SR, and intra-SR Ca^{2+} was recently found to increase the opening rate of the Ca^{2+} release channel in isolated, intact heart cells (Cheng et al. Science, in press). These results suggest that intraluminal Ca^{2+} content is also involved in channel regulation. We fused Ca^{2+} release channels of cardiac and skeletal muscle to lipid bilayers and directly assessed the effect of *trans* (intraluminal) $[Ca^{2+}]$ on open probability (Po). Cs^+ was used as the charge carrier and openings were elicited by the addition of 10 μM Ca^{2+} to the *cis* (cytoplasmic) side. Increasing luminal $[Ca^{2+}]$ from 0.1 to 10 mM increased Po of cardiac and skeletal channels by increasing mean open time and frequency of events. The higher selectivity for Ca^{2+} over Cs^+ was reflected as discrete reduction of unitary channel conductance (figure). When cytosolic $[Ca^{2+}]$ was reduced to 0.1 μM, similar increments of luminal $[Ca^{2+}]$ failed to increase Po significantly. Our results suggest the existence of an interactive regulation of channel activity by Ca^{2+} binding sites at both sides of the membrane. Supported by NIH and AHA.

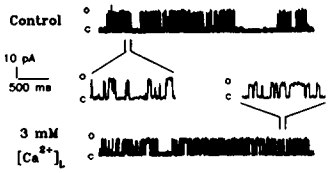

M-PM-A10

INTERACTION OF SITE-DIRECTED FKBP-12 MUTANTS WITH THE CALCIUM RELEASE CHANNEL OF RABBIT SKELETAL MUSCLE SARCOPLASMIC RETICULUM. ((Anthony P. Timerman#, Sebastian Barg#, Alice Marcy+, Greg Wiederrecht+, and Sidney Fleischer#)). Department Molecular Biology, Vanderbilt University#, Nashville, TN 37235; and Department Immunology Research, Merck Research Laboratories+, Rahway, NJ 07065.

The 12 Kd FK-506 binding protein (FKBP) is tightly associated with the calcium release channel (CRC)/ryanodine receptor of skeletal muscle terminal cisternae (TC) (Jayaraman et al., J. Biol. Chem., 267, 1992). We have described a gentle procedure to dissociate and reconstitute human recombinant FKBP from and to the CRC of TC. Functional assessment of control TC vs. either FKBP depleted or FKBP reconstituted TC vesicles suggest that FKBP stabilizes the closed conformation of the CRC (Timerman et al., J. Biol. Chem., 268, in press, 1993). In this study, we have examined the interaction of FKBP depleted TC with site-directed mutants of FKBP which vary with regard to: 1) FK-506 binding activity, and/or 2) peptidyl-prolyl isomerase (PPIase) activity. Our results indicate that site-directed mutants of FKBP which are deficient in either FK-506 binding and/or PPIase activity bind to FKBP depleted TC vesicles. The influence of FK-506 binding and PPIase activities of FKBP on the function of the calcium release channel can now be assessed. [NIH HL32711 (SF)]. [MDA (SF)].

MITOCHONDRIAL CHANNELS

M-PM-B1

PROTEINS THAT BIND THE YEAST VDAC CHANNEL OF THE MITOCHONDRIAL OUTER MEMBRANE ((E. Blachly-Dyson and M. Forte)) Vollum Institute for Advanced Biomedical Research, Oregon Health Sciences University, Portland, Oregon 97201. (Spon. by M. Forte)

The voltage-dependent anion channel of the mitochondrial outer membrane (VDAC) forms voltage-gated pores in the mitochondrial outer membrane which are thought to be responsible for the movement of metabolic intermediates between the cytoplasm and the intermembrane space (IMS). VDAC may be involved in regulation of cellular metabolism by interacting with proteins in both the cytoplasm and the mitochondrion. For example, the opening and closing of VDAC channels can be altered by a soluble protein of the IMS, known as the VDAC modulator, which has not been extensively characterized. In addition, VDAC is the binding site for hexokinase and glycerol kinase, which bind differentially to the surface of the mitochondrion, depending on the metabolic state of the cell. In order to identify additional proteins which may interact with VDAC to regulate its function, we have used the two-hybrid system. A gene encoding the DNA binding domain of a the yeast GAL4 transcriptional activator protein fused to the VDAC gene was introduced into yeast cells containing HIS3 and LacZ reporter genes. The reporter genes can be activated only when a second fusion protein containing a transcription activation domain binds the VDAC fusion protein. A library containing yeast genomic sequences fused to the GAL4 activation domain was introduced into the yeast cells containing the VDAC fusion protein, and transformants were identified in which both the HIS3 and lacZ reporter genes were activated when a library plasmid was co-expressed with the VDAC fusion plasmid. These transformants contain plasmids encoding proteins which may interact with the VDAC protein. These genes will be discussed.

M-PM-B2

SHAPE OF THE LUMEN OF THE MITOCHONDRIAL CHANNEL, VDAC, PROVIDED BY ELECTRON CRYSTALLOGRAPHY. ((C.A. Mannella, X.W. Guo, B. Cognon, E. Dolginova, P.R. Smith*)) Wadsworth Center for Laboratories and Research, Albany NY, 12201-0509; *Dept of Cell Biology, New York Univ School of Medicine

Projected density maps of VDAC arrays are obtained by computer averaging of low-dose electron micrographs of 2D crystals (embedded in vitreous ice or gold-glucose) formed by phospholipase A_2 treatment of outer membranes from Neurospora mitochondria. Angular relationships among the 3 non-symmetry-related channels in the crystal cell have been determined and used to compute the projected density of a single channel. The wall forming VDAC's lumen contains four sites of low density. Three dimensional reconstruction (from images of tilted, gold-glucose-embedded crystals) shows that the density minima correspond to irregular features in the lumen wall, i.e. uneven height, and interior corners and grooves. Thus, the lumen's shape deviates significantly from a simple right-circular cylinder. A diagonal groove defines a "flap" in the sector of the lumen wall involved in a structural change induced by a modulator (König's polyanion). Sequence-specific antibodies (Stanley et al., this meeting) are being used to map segments of the VDAC polypeptide into the molecular envelope of the channel. (Supported by NSF grant MCB9219353.)

M-PM-B3

CIRCULAR DICHROISM OF ISOLATED MITOCHONDRIAL CHANNEL PROTEIN, VDAC: FIRST DIRECT EVIDENCE FOR PORIN-LIKE SECONDARY STRUCTURE. ((L. Shao, P. Van Roey, K. Kinnally, C.A. Mannella)) Wadsworth Center for Laboratories and Research, Albany NY, 12201-0509

The 31-kDa VDAC polypeptide has been purified from Neurospora mitochondria by hydroxylapatite chromatography in the presence of LDAO (DePinto et al, 1989, Eur J Bioch 183:179). Circular dichroism (CD) spectra have been recorded from the VDAC protein in 2% β-octyl glucoside (βOG) and in liposomes (92% phosphatidylcholine, 8% phosphatidic acid). Lipid-reconstituted VDAC shows good pore-forming activity, as measured by both light scattering and electrophysiological assays. CD spectra of VDAC were recorded from 184 to 260 nm in βOG suspensions, and from 200 to 260 nm in liposomes. The spectra of VDAC in βOG and in liposomes over the latter range are similar, suggesting that the channel's secondary structure is not dramatically different in micelles of this detergent and in lipid bilayers. The CD spectrum of VDAC in βOG is almost identical to that of bacterial porin in the same detergent (Markovic-Housley & Garavito, 1986, Biochim Biophys Acta 869:158). While β-barrel models for VDAC have been proposed since 1987 based on sequence analysis, this is the first physical evidence that VDAC has extended β-sheet structure like the porins. (Supported by NSF grant MCB9219353.)

M-PM-B4

USE OF SEQUENCE-SPECIFIC ANTIBODIES TO PROBE THE TOPOLOGY OF THE VDAC CHANNEL PROTEIN IN THE MITOCHONDRIAL OUTER MEMBRANE. ((S. Stanley, J.A. Dias, G. Bazinet, G. Waterman, M. Vercolon, C.A. Mannella)) Wadsworth Center for Laboratories and Research, Albany NY, 12201-0509

Specific anti-peptide antibodies have been obtained by immunizing rabbits with four different amino-acid segments of the VDAC protein of N. crassa: 1-20 (N-terminus), 195-210, 251-268, and 272-283 (C-terminus). The antisera bind to VDAC in either Western blots or lysed mitochondria. Reactivity of antisera with suspended mitochondria before and after deliberate lysis were compared by enzyme-linked colorigenic assays. These results indicate that both the N- and C-terminal peptide epitopes are exposed on the inside-facing surface of the outer mitochondrial membrane. First results suggest that the 195-210 segment also faces inside while 251-268 faces out. The effects of modulators of VDAC activity on antibody binding are also being studied. Preincubation of lysed mitochondria with a crude soluble mitochondrial protein fraction (which should contain VDAC modulator protein: Holden & Colombini, 1988, FEBS Lett, 241:105) inhibits antisera binding to both N- and C-termini. König's polyanion (5 μM) most strongly inhibits antibody binding to the 251-268 region. (Supported by NSF grants MCB9219353, BBS9101291, DIR8914757.)

M-PM-B5

NADH CONTROLS MITOCHONDRIAL RESPIRATION BY REGULATING THE OUTER MEMBRANE PERMEABILITY TO ADP. ((A. Lee, M. Zizi, M. Colombini)) Dept. Zoology, Univ. Maryland, College Park, MD 20742.

VDAC is presumed to be the main pathway through which substrates and metabolites cross the mitochondrial outer membrane (OM). It forms a large aqueous pore which is voltage-gated. Recently, the cofactor, ß-NADH, has been shown to selectively increase the voltage dependence of the channel (K_D=16 μM). Other nucleotides tested were without effect. We devised a novel approach to obtain the permeability of the mitochondrial membranes for ADP by using polarographic data. By applying this methodology to intact mitochondria isolated from potato tubers, ß-NADH, at micromolar concentrations, is found to decrease the OM permeability to ADP by a factor of 4 to 6 fold. The effect was highly selective as NAD^+ displayed only 2% of the NADH effect. The effect correlated with the OM intactness. When conditions were controlled to inhibit the ß-NADH dehydrogenase enzyme located at the cytoplasmic face of the inner membrane, these did not diminish the NADH-induced decrease in OM permeability. α-NADH, which is known to stimulate a dehydrogenase on the OM, displayed only 10% of the activity of the ß form of the cofactor. This would be consistent with this enzyme not being involved since the commercially available α form is contaminated by the ß form. These data confirm that the glycolytic ß-NADH can regulate mitochondrial respiration by altering the OM permeability through the VDAC channel. (Supported by ONR grant # N00014-90-J-1024)

M-PM-B6

EIGHT MONOCLONAL MOUSE ANTI-"PORIN 31HL" ANTIBODIES DISCRIMINATE BETWEEN HVDAC1 AND HVDAC2.
F.P.Thinnes, C.Morys-Wortmann, N.Hilschmann. Max-Planck-Inst.f.exp.Medizin; Hermann-Rein Str.3, D-37075 Göttingen (Spon.by H.Tedeschi)

1991 we reported on the characterization of eight monoclonal mouse antibodies raised against highly purified human VDAC "Porin 31HL"; concerning epitope specificity all eight mAbs equally reacted with the N-terminus of human porin (Babel et al., Biol.Chem.Hoppe-Seyler 372,1027,1991). Now, we present first data indicating that our anti-"Porin 31HL" antibodies discriminate between HVDAC1 and HVDAC2. Basing on the data of Blachly-Dyson et al. (J.Biol.Chem.268,1835,1993) we synthesized various peptides of the N-terminus of HVDAC2. In dot blots on nitrocellulose or PVDF these HVDAC2-type peptides do not react with our anti-"Porin 31HL" antibodies, while HVDAC1-type peptides of corresponding size are clearly labelled. We are on the way to scrutinize these data by ELISA tests. The data strongly support our immuno-topological data on the expression of "Porin 31HL", which is HVDAC1-type, in the plasmalemma of human B lymphocytes which we meanwhile confirmed on the electron microscopy level by the application of our mouse mAbs (Cole et al.,Biol.Chem.Hoppe-Seyler 373,891,1992).

M-PM-B7

VOLTAGE SENSING BY THE CYCLOSPORIN A-SENSITIVE PERMEABILITY TRANSITION PORE OF MITOCHONDRIA INVOLVES CRITICAL THIOL GROUPS.
((V. Petronilli and P. Bernardi)) CNR and Department of Biomedical Sciences, University of Padova, 35121 Padova, Italy (Spon. by D. Pietrobon)

Mitochondria possess an inner membrane channel, the permeability transition pore (MTP), which is inhibited by Cyclosporin A. The pore is a channel modulated by (i) the membrane potential, with an increase of the open probability upon depolarization [1,2] and (ii) matrix pH, with a decrease of the open probability upon matrix acidification through protonation of critical histidyl residues [3]. We have recently shown that many physiological effectors, including Ca^{2+} ions, directly affect the pore voltage sensing rather than the membrane potential *per se* [4]. Here we show that MTP opening by a series of thiol reagents (phenylarsenoxide, arsenoxide, menadione, *t*-butylhydroperoxide) is inhibited by the alkylating agent N-ethylmaleimide (NEM) with Ki ≅ 2 μM. The effect of the thiol reagents is related to a shift of the gating potential to higher values, which is fully reversed by micromolar NEM concentrations. These findings suggest that critical thiol groups play a role in the regulation of voltage sensing by the MTP.

[1] Bernardi P (1992) J Biol Chem 267, 8834
[2] Petronilli V, Cola C, Bernardi P (1993) J Biol Chem 268, 1011
[3] Nicolli A, Petronilli V, Bernardi P (1993) Biochemistry 32, 4461
[4] Petronilli V et al (1993) J Biol Chem 268 (Oct-Nov), in press

M-PM-B8

DOES VDAC FORM PART OF THE ORDIC CHANNEL COMPLEX?
F.P.Thinnes, M.Heiden, H.Flörke, N.Hilschmann. Max-Planck-Inst.f.exp.Medizin; Hermann-Rein Str.3, D-37075 Göttingen (Spon.by C.A.Mannella)

We reported on the expression of VDAC in the plasmalemma of human B lymphocytes (Thinnes et al., Biol.Chem.Hoppe-Seyler 370,1253,1989). Corresponding results for human surface epithelial respiratory cells showed colocalization of VDAC and CFTR in the apical domain of SERC (Puchelle et al., Biol.Chem.Hoppe-Seyler 374,297,1993), data fitting to ORDIC being under control of CFTR. We demonstrated that cytosolic fractions alter channel characteristics of human VDAC in lipid bilayers (Heiden et al., Biol.Chem.Hoppe-Seyler 374,149, 1993). Cytosolic modulators of ORDIC are in debate since 1989. We showed that anti-porin antibodies block endothelial Cl^- channels (Janisch et al., Arch.Pharmacol.347, Suppl.,R73,1993). We presented first data on binding of ATP or Stilbene-Disulfonate by VDAC, agonists which regulate ORDIC (Thinnes et al., North Amer. CF Conference, Washington,D.C., Oct.1992). We meanwhile corroborated and will discuss both traits of VDAC (Flörke et al.,in prep.). Porin channels in the plasmalemma thus share several traits with ORDIC in Cystic Fibrosis epithelial cells which will be summarized.

M-PM-B9

PATCH-CLAMPING OF YEAST MITOPLASTS

((Timothy Lohret and Kathleen Kinnally)) Department of Biological Sciences, SUNY at Albany, Albany, New York 12222 and Wadsworth Center for Laboratories and Research, NYS Dept. of Health, Albany, New York 12201.

Patch-clamping of the inner mitochondrial membrane has identified several distinct channel activities. One of these is characterized by a variety of conductance levels, some as high as 1.5 nS and has been previously described in detail (Kinnally et. al (1992) J. Bioenerg. Biomembr. 24, 99). We have found a similar activity in mitoplasts generated from yeast mitochondria. Comparable characteristics in the wild-type include similar conductance levels (observed levels include 50 pS, 500 pS, 1.2 nS, as well as several other levels), voltage activation, and voltage dependence. The sensitivity of MCC activity to ligands of the mitochondrial benzodiazepine receptor in rat heart(Kinnally et al.(1993) P.N.A.S. 90, 1374) suggests an involvement of VDAC in this activity. In order to test this idea we have compared the channel activity recorded from mitoplasts in wild-type yeast and a VDACless mutant strain M22-2 courtesy of M. Forte and E. Blachly-Dyson (Blachly-Dyson et al. (1989) Science 247, 1233-1236). The activity of the two were found to be comparable in the membrane potential range of $\pm$40mV. Some preliminary experiments, however, indicate that the voltage dependence at higher negative potentials is altered in the mutant, consistent with a possible role of VDAC. In addition, a 50pS slightly anionic channel activity independent of MCC activity is seen in both wild-type and VDAC-less mitoplasts. This study was supported in part by National Science Foundation Grant MCB 9117658.

M-PM-B10

A PATCH-CLAMP STUDY OF THE CATIONIC CHANNEL OF MITOCHONDRIA

((M.Zoratti, I.Szabo', G.Bathori, T.Starc, D.Wolff and G.Schatz[1])) CNR Unit for the Physiology of Mitochondria, Padova, Italy and [1]Biozentrum, Basel, Switzerl.

Porin-less yeast mitochondria have proven ideal for the study of a channel present also in wild-type yeast and rat liver mitochondria. Its main features are the following: 1) It can operate in several conductance states in the 100-600pS range (100 mM KCl). 2) The occupancy of the substates depends on the applied potential. 3) In excised patches the channel is strongly voltage-dependent, with negative potentials favoring the open state(s). In the cell-attached configuration, the voltage dependence is weaker and of the opposite sign. 4) In excised patches the response to voltage pulses from zero holding potential is described by one exponential: the time constants of the inactivation process range from 7 (60mV) to 220 (10mV) ms, while for activation the τ's range from 1100 (-10mV) to 450 (-60mV) ms. 5) The channel is cationic, with P_K/P_{Cl} about 6. 6) It was observed in the outer and inner membrane fractions as well as in the contact sites fraction of yeast mitochondrial membranes. 7) In bilayer experiments, the addition of mitochondrial leader peptide (courtesy of Prof. J.P. Henry) induced fast flicker. We believe that this channel can be identified with the "peptide sensitive channel" described by Thieffry et al. (EMBO J. 7, 1449-54 (1988)), and that it might coincide with the activities reported by Dihanich et al. (Eur. J. Biochem. 181, 703-708 (1989)) and by Tedeschi et al. (J.Membr. Biol. 97, 21-29 (1987)) in bilayer and patch-clamp work, respectively, on the mitochondrial outer membrane.

M-PM-B11

RESPIRATORY UNCOUPLERS AFFECT MITOPLAST CHANNEL ACTIVITY

((Maria Luisa Campo*, Kathleen W. Kinnally†, Henry Tedeschi‡)) *Dpto. Bioq. y Biol. U. de Extremadura, Caceres, Spain, †Wadsworth Center for Labs & Res., NYS Dept. of Health, Albany, NY, ‡Biology Dept. SUNY Albany, Albany, NY

Patch-clamp techniques were used to record the channel activities from mouse liver mitoplasts (mitochondria treated to remove the outer membrane). The present report shows that uncouplers of the respiratory chain like FCCP (Carbonyl cyanide *p*-trifluoromethoxyphenyl hydrazone) and CCCP (Carbonyl cyanide *m*-chlorophenyl hydrazone) perturb the two predominant channel activities, MCC (Multiple Conductance Channel) and mCS (mitochondrial Centum picoSiemen). In general, micromolar levels of these effectors increase the open probability of MCC. In contrast, there is a general inhibition of mCS at similar concentrations. The uncoupler effects were reversible in about half of the patches. The uncoupler binding site(s) responsible for the perturbation of channel activities are probably distinct from those sites involved with uncoupling oxidative phosphorylation since effects on respiration are observed at lower concentrations. Nevertheless, current work examining the effect of metabolic inhibitors (Campo et al., 1992, J. Biol. Chem., **267**, 8123) and uncouplers are not only increasing our understanding of mitochondrial channels but also must be considered in metabolic studies. This study was supported in part by National Science Foundation grant MCB9117658.

K CHANNELS I

M-PM-C1

ACTIVATION MODEL FOR WILD-TYPE AND V2 MUTANT *SHAKER* POTASSIUM CHANNELS.

((N.E. Schoppa and F.J. Sigworth)) Dept. Cell. and Molec. Physiology, Yale Univ., New Haven, CT 06510. (Spon. by B.A. Davis)

The V2 mutation, corresponding to L382V in the *Shaker* B sequence, shifts the voltage dependence of activation in *Sh* 29-4 channels by +60 mV (McCormack et al., *PNAS* **88**, 2931 (1991)) while shifting the voltage dependence of only a part of the charge movement (Schoppa et al., *Science* **255**, 1712 (1992)). To account for most of the kinetic properties of the wild-type (WT) and V2 channels, we propose a model of the activation process in which the channel opens following two sequential transitions within each subunit and a final concerted conformational change:

$$(S_0 \leftrightarrow S_1 \leftrightarrow S_2)_4 \leftrightarrow O \leftrightarrow C$$

The transitions $S_0 \leftrightarrow S_1$ and $S_1 \leftrightarrow S_2$ within a subunits proceed independently of the state of the other subunits. The rates of these transitions are constrained largely by measurements of gating and macroscopic ionic currents measured over a broad voltage range (-140 to +180 mV). The voltage dependence of each of these transitions corresponds to ~1 to 1.5 elementary charges, most of it associated with the backward rates. The inclusion of a distinct final transition to the open state final reflects the fact that the channel closing rate, as seen in the tail currents at asymptotically low voltages, is relatively slow and has a small associated valence (~0.4 e_0), while the channel reopening rate, observed during channel reactivation following very short hyperpolarizations, is very fast ($\tau \approx 0.1$ ms at +60 mV). The presence of multiple tail current components in the V2 and WT channel, and the V2 single channel bursting behavior, is also consistent with a fast channel reopening rate. The main effect of the mutation appears to be an acceleration of the transitions $S_1 \leftarrow S_2$ and $(S_2)_4 \leftarrow O$.

M-PM-C2

GATING CURRENT FLUCTUATIONS IN *SHAKER* K+ CHANNELS.

((Y. Yang and F. J. Sigworth)) Department of Cellular and Molecular Physiology, Yale School of Medicine, New Haven CT 06510.

If gating currents arise from discrete charge movements, they are expected to contain nonstationary "shot" noise. The figure shows the mean current and time dependence of the variance from an ensemble of 8400 gating current responses from W434F-mutant *Shaker* channels with depolarizations to +40 mV (5 kHz bandwidth). Also shown is the auto-covariance function $C(t_1,t_2)$ plotted as a function of t_2 (t_1 is fixed at the time of peak "off" gating current). Superimposed are the predictions of a 17-state kinetic model (see abstract by N. E. Schoppa and F. J. Sigworth). Qualitative features of the variance and covariance are well predicted. Quantititive discrepancies will be discussed.

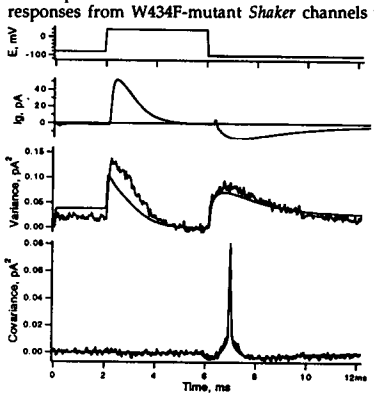

M-PM-C3

THE CALCIUM SENSITIVITY OF TWO K_{CA} CHANNELS IS PARTIALLY DETERMINED BY A SEPARABLE C-TERMINAL DOMAIN. ((C.R. Solaro*, A. Wei#, C.J. Lingle#* and L. Salkoff#+)) *Dept. of Anesthesiology, #Dept. of Anatomy and Neurobiology and +Dept. of Genetics, Washington Univ. Sch. of Med., St. Louis, MO 63110.

A comparison of the large-conductance calcium-activated potassium channel (mSlo) encoded by a recently cloned mouse gene (Butler et. al., Science 261: 221-4, 1993) with the homologous *Drosophila* channel, slopoke (fSlo) (Adelman et. al., Neuron 9: 209-16, 1992), reveals two highly conserved domains which are linked by a relatively non-conserved stretch of amino acids. The first domain, which includes eight hydrophobic segments (S1-S8) and a putative pore region, resembles the core of other voltage-gated potassium channels. The second domain, which includes hydrophobic segments S9 and S10, forms a large C-terminal extension not found in voltage-gated channels. RNA transcripts encoding only the mSlo "core" region (S1-S8) do not produce functional channels in Xenopus oocytes; however, active channels are produced when separate transcripts encoding both the core and mSlo "C-terminal" (S9-S10) domains are coinjected. Thus, mSlo channels are composed of two separable domains. Recordings from inside-out patches show that channels produced by coexpression of the two domains have conductance, kinetics, voltage- and calcium-sensitivity similar to channels encoded by the full-length mSlo transcript. The fSlo channel, although similar in structure to mSlo, has a markedly lower calcium sensitivity and faster gating kinetics. Given these differences, we investigated the influence of the C-terminal domain on channel function by coinjecting core and C-terminal transcripts from both mSlo and fSlo to form heterologous channels. Coinjection of the mSlo core with the fSlo C-terminal transcript produced channels with gating kinetics similar to mSlo but with lower calcium (Ca^{2+}) sensitivity than mSlo (half-activation voltage (V_{50}) shifted positive by 30 mV at 10 μM Ca^{2+}). Conversely, coexpression of the fSlo core domain with the mSlo C-terminal transcript produced channels with gating kinetics similar to those of fSlo, but with a higher calcium sensitivity than fSlo (V_{50} shifted negative by > 67 mV at 10 μM Ca^{2+}). Thus, the C-terminal domain partially determines calcium sensitivity while conductance and kinetics are largely determined by the core domain.

M-PM-C4

MUTATIONAL ANALYSIS OF THE INNER MOUTH OF THE PORE IN DELAYED RECTIFIER K^+ CHANNELS.

((C.-C. Shieh, J.A. Drewe, A.M. Brown and G.E. Kirsch)) Departments of Anesthesiology, and Molecular Physiology and Biophysics, Baylor College of Medicine, Houston, TX 77030. (Spon. by A.M. Brown)

Two cloned potassium channels from rat brain, Kv2.1 and Kv3.1, differ in single channel conductance and sensitivity to block by external tetraethylammonium (TEA), internal TEA and internal 4-aminopyridine (4-AP). To identify the regions responsible we constructed six chimeric channels in addition to the previously described S5-S6 linker chimera. In each construct a segment of Kv3.1 in the post-S4 C-terminus region replaced the equivalent segment of the host, Kv2.1. Electrophysiological analysis of channels expressed in *Xenopus* oocytes, showed whereas the S5-S6 chimera had a single channel conductance increase of about 3-fold, the six new chimeras had only modest changes in conductance (±50%) and no change in external TEA block. However in the 5'S5 and 3'S6 chimeras which mutate the putative cytoplasmic halves of S5 and S6 respectively, sensitivities to internal blockers changed to more closely resemble those of the donor Kv3.1 channel. Point mutations of Kv2.1 at each of four non-conserved positions in the cytoplasmic half of S6 revealed that L403M and I405V, respectively, were responsible for the internal TEA and 4-AP blocking characteristics of the 3'S6 chimera. We conclude that for Kv 2.1 and Kv3.1 the S5-S6 linker is a major determinant of ion conduction and external TEA block, while the 5'S5 and 3'S6 form part of the inner mouth of the pore. (Supported by NIH grants NS29473 and NS23877).

M-PM-C5

TRANSFER OF TOXIN SENSITIVITY FROM A KV1 TO A KV2 POTASSIUM CHANNEL. ((Adrian Gross and Roderick MacKinnon)) Department of Neurobiology, Harvard Medical School, Boston, MA 02115.

The Kv1.3 potassium channel is inhibited by low concentrations of charybdotoxin and many of its isoforms. In contrast, Kv2.1 is completely insensitive to these toxins. By transferring the stretch of amino acids between S5 and S6 from Kv1.3 to Kv2.1, the modified Kv2.1 channel acquires toxin sensitivity. To identify residues responsible for the extreme difference in sensitivity between Kv1.3 and Kv2.1, we first subdivided the transferred region into three roughly equal parts. None of these smaller stretches conferred toxin sensitivity alone. Both outermost parts were required for the transfer of sensitivity. Using site-directed mutagenesis, we identified two crucial residues on Kv1.2 (two lysines, one in each of the outermost parts) that could confer toxin sensitivity when replaced with small, apolar residues. These results are consistent with earlier studies on the Shaker potassium channel and further suggest that regions outside the S5-S6 linker probably do not interface with the toxin when it is bound.

M-PM-C6

CHARYBDOTOXIN AS A STRUCTURAL PROBE OF *SHAKER*: COMPLEMENTARY MUTAGENESIS AND ELECTROSTATIC DISTANCE GEOMETRY. ((C. Miller, M. Stocker, and S.A.N. Goldstein)) HHMI, Graduate Dept. of Biochemistry, Brandeis University, Waltham, MA.

A method is introduced to estimate distances between residues in the external mouth of a *Shaker* K^+ channel, using charybdotoxin (CTX), a peptide blocker of known structure. Certain residues in the CTX receptor domain act purely via through-space electrostatic energies: the residue's charge, but not its chemical structure, influences CTX binding affinity. For such a residue, the "electrostatic compliance," σ_{ij}, is a direct measure of the distance, r_{ij}, between residue i on the toxin and j on the channel:

$$\sigma_{ij} \equiv \frac{\partial^2 \Delta G^\circ}{\partial z_i \partial q_j} = f(r_{ij}),$$

where ΔG° is the free energy of toxin binding, and z_i, q_j the valences of a chosen pair of residues on toxin and channel, respectively. The function $f(r_{ij})$ describes the distance-dependence of the charge-charge interaction energy between the i and j residues. A single value of σ_{ij} is derived from ΔG° of toxin binding measured on a matrix of at least 9 channel-toxin mutant pairs, with charges of -1, 0 and +1 each at toxin residue i and channel residue j. A first test of this approach focuses on *Shaker* Lys427 and several residues of CTX. The K_D for wild-type CTX varies from 1 to 70 pM as charge at *Shaker* residue 427 varies from -1 to +1. This dependence of CTX binding on q_{427} is insensitive to toxin charge at residue 24 but is strongly sensitive to charge at residue 11. Thus, *Shaker*-427 is far away from position 24 on bound CTX ($\sigma_{ij} \sim 0$), but close to CTX position 11 ($\sigma_{ij} \sim 2.5$ kJ/mol).

After the customary hand-waving about dielectric interfaces, we estimate distances between *Shaker* residue 427 and CTX residues 24 and 11 as >18 Å and <6 Å, respectively. This result places *Shaker* residues Lys427 and Thr449 about 15 Å apart. Further work is aimed at *Shaker* residue 422, another electrostatic residue.

M-PM-C7

MAPPING THE CTX AND NTX BINDING SITES ON THE Kv1.3 POTASSIUM CHANNEL. ((J. Alyar, M. Simon-Steel, S. Burrows, B. Dethlefs, K. G. Chandy)). Dept. of Physiol. & Biophys., UC Irvine, CA 92717.

Using site-specific mutagenesis we have identified several residues that influence charybdotoxin (CTX) and noxiustoxin (NTX) block of the Kv1.3 channels.

P-REGION

Kv1.3 378 SSGFNSIPDAFWWAVVTMTTVGYGDMHPVT 407

Replacement of G380 with H confers resistance to CTX, but not to NTX. Substitution with a larger residue (G380F) makes Kv1.3 resistant to NTX as well. Thus, residues larger than glycine at position 380 probably prevent these toxins from accessing their binding sites. Mutations at H404 influence CTX and NTX-block in a size-dependent manner, while positively charged residues render the channel CTX- and NTX-resistant, probably via charge repulsion. Protonation of the native H404 reduces sensitivity to CTX, making the channel resistant to CTX block at pH 6.0. This pH-effect is not due to protonation of histidines in CTX, because the toxin blocks the H404T mutant at pH's ranging from 7.6 to 6.0 with the same potency. Mutants V406D and T407A exhibit faster inactivation in parallel with a reduction of toxin block. In contrast to previous reports, mutation of aspartate 386 (D386N/E/I), the residue that corresponds to D431 in *Shaker*, did not alter CTX or NTX binding. Our data suggest that glycine 380 lines the entryway to the toxin binding sites, which lie close to H404, probably involving D402. The role of D402 could not be tested since D402N/E mutations produce non-functional channels. Supported by grants from AHA (#92-59, J.A) and Pfizer Inc (K.G.C).

M-PM-C8

STRUCTURAL CHANGES IN THE OUTER MOUTH OF K^+ CHANNELS ACCOMPANYING C-TYPE INACTIVATION. ((Gary Yellen, Deborah Sodickson, Tsung-Yu Chen and Mark Jurman)) Dept. of Neurobiology, Harvard Medical School and Mass. General Hospital, Boston, MA 02114.

Substitution of a cysteine in the extracellular mouth of the pore of the Shaker-IR K^+ channel permits allosteric inhibition of the channel by Zn^{2+} or Cd^{2+} ions at micromolar concentrations. Cd^{2+} binds weakly to the open state but drives the channel into the slow (C-type) inactivated state, which has a K_d for Cd^{2+} of roughly 0.2 μM. There is a 45,000-fold increase in affinity when the channel changes from open to inactivated. These results indicate that C-type inactivation involves a structural change in the external mouth of the pore, consistent with our earlier finding that external TEA slows C-type inactivation. This structural change is reflected in the T449C mutant as state-dependent metal affinity, which may result either from a change in proximity of the introduced cysteine residues of the four subunits, or from a change of the exposure of this residue on the surface of the protein, or both. We have tested for a change in surface exposure using a sulfhydryl-specific chemical reagent. Chemical modification of the cysteines with methyl methanethiosulfonate abolishes the sensitivity to Cd^{2+}; this modification proceeds much faster if the channel is in the inactivated state, indicating that the introduced cysteine at position 449 becomes more exposed upon inactivation. This picture fits nicely with the pattern with which mutations at this site affect the C-type inactivation rate.

M-PM-C9

PROBING THE MOUTH OF A K⁺ CHANNEL BY A SULFHYDRYL-SPECIFIC REAGENT AFTER CYSTEINE SUBSTITUTION MUTAGENESIS

((L.L. Kürz, H.-J. Zhang, R.D. Zühlke and R.H. Joho)) Department of Cell Biology and Neuroscience, The University of Texas Southwestern Medical Center, Dallas, TX 75235-9111

The segment between S5 and S6 of voltage-gated K⁺ channels, called H5 or P region, has been implicated to form part of the ion conduction pathway. Little is known about the conformation of this region although various models have been proposed including a ß barrel-like structure formed by four adjacent antiparallel ß sheets. To gain insight into the secondary structure of this region, we used cysteine substitution mutagenesis and sulfhydryl-specific, membrane-impermeant reagents to probe the accessibility of amino acid side chains in and around the P region of Kv2.1 (DRK1). Twenty-eight positions from K356 to T383 were each mutated to a cysteine. After expression of mutant K⁺ channels in *Xenopus* oocytes, cysteine side chain accessibilities were probed by superfusion with $CH_3SO_2SCH_2CH_2NMe_3^+$ (MTSET). MTSET can form a mixed disulfide with an accessible cysteine, and this may lead to current reduction if the covalently modified side chain is in or close to the ion conduction pathway. Thus far, we have identified four mutations that showed K⁺ current reduction after superfusion with 3 mM MTSET. The mutants P361C, I379C, Y380C, and K382C showed 87%, 99%, 39%, and 21% reduction in current amplitude, respectively. In contrast, mutants S363C, A367C, T368C behaved like wild type Kv2.1 with less than 5% current reduction. Our results suggest that the side chains of P361, I379, Y380, and K382 are directly accessible from the extracellular environment. Taken together, these residues may, therefore, face the lumen of the ion channel pore. Furthermore, the degrees of inhibition are in agreement with a model in which the ion conduction pathway narrows from residue K382 to Y380 to I379. (Supported by NIH grant NS28407 and a grant of The Muscular Dystrophy Association to R.H.J.)

M-PM-10

MOLECULAR DISSECTION OF A K⁺ CHANNEL T1 DOMAIN INTO SUBDOMAINS.

N.V. Shen* and P.J. Pfaffinger, Div. of Neuroscience, BCM, Houston, TX 77054

Recently, Li et al (1992) and Shen et al (1993) have shown that the N terminal domain (T1) plays a critical role in the assembly of Shaker type K⁺ channel subunits. In addition, this T1 domain is able to self tetramerize, and may also confer subfamily specificity. To test sequences within the T1 domain important for multimerization and subfamily specificity, we have constructed a family of chimeric T1 domains, using the Shaker type AKv1.1a (1.1) and Shaw type AKv3.1a (3.1) clones. Sequence analysis shows three conserved subdomains, which we have designated A, B, and C. We designed chimeric 1.1 T1 domains by engineering in novel restriction sites between subdomains and substituting in 3.1 subdomains: 3A1BC (3A, for 3.1 subdomain A, 1BC for 1.1 subdomains B and C), 1A3B1C, 1AB3C, and control constructs, called 1ABC and 3ABC. We tested synthesized chimeric T1 domain proteins for stable self-tetramerization by sucrose gradient centrifugation analysis. The rescue constructs, 1ABC and 3ABC, were able to form stable tetramers, behaving like wild type 1.1 and 3.1 N terminal domains. The chimeric proteins (3A1BC, 1A3B1C, and 1AB3C) ran as monomers on sucrose gradients, suggesting an inability to homomultimerize. We next tested these chimeric T1 domains for assembly with the wild type 1.1 tagged N terminal domain (1T1-tag 1) by a co-immunoprecipitation assay. 1T1-tag 1 co-precipitated 1AB3C, not 3A1BC or 1A3B1C. To test if the C subdomain is necessary for multimerization with 1T1-tag1, we deleted the C subdomain from the T1 domain rescue construct. This protein, called 1AB, failed to co-precipitate with the wild type T1 domain and ran as a monomer on sucrose gradients. These results suggest that substitution of any 3.1 subdomain into the 1.1 T1 domain disrupts stable self-tetramerization of the protein. Finally, although a C subdomain is required for asssembly, function can be partially restored by substitution of 3C for the 1C subdomain of 1.1 T1, which allows heteromultimerization with the wild type T1 domain. *Supported by NIH RO1-NS 31583, Baylor Mental Retardation Center P30-HD24064, Klingenstein Fellowship Award, NRSA F30 MH10511*

DNA STRUCTURE

M-PM-D1

A TRUNCATED OCTAHEDRON BUILT FROM DNA USING SOLID-SUPPORT METHODOLOGY.

((Yuwen Zhang and Nadrian C. Seeman)) Department of Chemistry, New York University, New York, NY 10003.

A covalently closed molecular complex whose double helical edges have the connectivity of a truncated octahedron has been assembled from DNA. This 3-connected Archimedean solid contains six squares and eight hexagons, formed from 36 edges arranged about 24 vertices. The vertices are the branch points of 4-arm DNA junctions, so each vertex has an extra exocyclic arm associated with it. The construct contains six single stranded cyclic DNA molecules that form the squares and the extra arms; in addition, there are 8 cyclic strands that correspond to the 8 hexagons. Each edge contains two turns of double helical DNA, so that the 14 strands form a catenated structure in which each strand is linked twice to its neighbors along each edge. Synthesis is proved by demonstrating the presence of each square in the object, and then by confirming that the squares are flanked by tetracatenane substructures, corresponding to the hexagons.

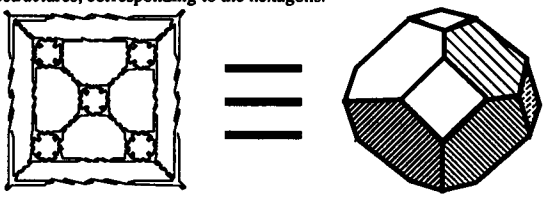

Supported by grants from ONR, NIH and W.M.Keck.

M-PM-D2

THREE-WAY DNA JUNCTIONS ARE STRONGLY BENT: CYCLIZATION STUDIES

((L. S. Shlyakhtenko[1,2,5], E. Appella[3], I. Kutyavin[4], R.E. Harrington[5] and Y. L. Lyubchenko[2]))
[1]SRI International, 333 Ravenswood Avenue, CA 94025, [2]Dept. of Microbiology, Arizona State Univ., Tempe, AZ 85287, [3]MicroProbe Corp., Bothell, WA 98021, [4]NCI, NIH, Bethesda, MD 20892, Dept. of Biochem., [5]UNR, Reno, NV 89557

We studied the geometry of three-way DNA junctions with a short hairpin as a third arm placed between two linear arms. Sticky ends at the ends of linear arms allow multimer formation during ligation. Ligated product contains rather short circular molecules which are separated from the linear ones by use of two-dimensional gel electrophoresis. Angles between arms were estimated from the circles sizes. It was shown that the hairpin induces severe bend between linear arms, so that the angle as small as 60° between arms can be formed. The irregularities in base pairing at branch point (mismatches, bulge) dramatically change the static and dynamic structural characteristics of the 3-way junctions. Mismatches stabilize severely bent geometry of the junction. Effect is qualitatively similar for bulges. The geometry of a 3-way junction depends also on its nucleotide composition. The molecule with the same G+C content in all branches adopt rather symmetrical geometry.

M-PM-D3

ION-INDUCED STABILIZATION OF THE G-DNA QUADRUPLEX : FREE ENERGY PERTURBATION STUDIES

((Wilson S. Ross[1] and Charles C. Hardin[2])) [1]Department of Pharmaceutical Chemistry, University of California, San Francisco, CA 94143 and [2]Department of Biochemistry, North Carolina State University, Raleigh, NC 27695.

Free energy perturbation / molecular dynamics calculations were used to determine how the size of an internally bound monovalent cation affects the stability of an antiparallel G-DNA quadruplex in water. A free energy cost was incurred as the cation size was increased in both water and within the DNA 'host' complex. However, in water the free energy tended to level off as the ionic radius increased and charge density decreased. In contrast, in the DNA complex the free energy became progressively larger as the cation began to induce conformational deformations in the relatively constrained octahedral carbonyl oxygen binding site. The minimum point in the energy curve obtained by subtracting the two resulting free energy curves indicates the favored cation for binding within the complex. Two sets of ionic Lennard-Jones '6-12' van der Waals parameters were tested and gave similar results. In both cases the minimum free energy is in the middle of the size range of the monovalent monoatomic cations, in qualitative agreement with experimental results. Changing the effective internuclear radius between the guanine carbonyl oxygen (O6) atoms and the bound cation resulted in a closer match to the experimental trends in ion-dependent quadruplex stabilization (i.e. $K^+ > Na^+$), suggesting that the larger ions may be smaller in the complex than in water. An antiparallel closed-loop model for the DNA sequence $d(T_2G_4)_4$ was also constructed by adding two covalently connected thymidine residues to close each major groove at one end of the quadruplex stem and each minor groove at the other end. Inter-loop thymidine-thymidine base pairing interactions formed at each end in dynamics starting from several different initial loop configurations.

M-PM-D4

THE MAGNITUDE AND DIRECTION OF CURVATURE OF GGGCCC CONTAINING DNA FRAGMENTS AS DETERMINED BY CIRCULARIZATION ASSAYS

Mensur Dlakic and Rodney E. Harrington, Department of Biochemistry, School of Medicine, University of Nevada Reno, Reno NV 89557-0014 USA

Although all DNA sequences contribute to DNA wrapping around the nucleosome core, DNA curvature is generally associated only with properly phased tracts of adenines. This apparent contradiction arises because the curvature of DNA sequences lacking adenine tracts is only weakly detectable by conventional gel mobility assays. Recent studies have shown that the GGCC motif is strongly curved as evidenced by Dnase I cutting, phasing analysis with adenine tracts and X-ray crystallography. In the present work, we have employed DNA circularization assays to determine the upper limit of curvature as 30 degrees per helical repeat in the GGGCCC motif. In addition, this sequence seems to exhibit exceptional torsional flexibility since small changes in the helical repeat of the basic oligomer used for cyclization did not lead to significant differences either in occurrence or in distribution of ring sizes. Our observations, together with recent reports on the substantial influence of divalent cations on curvature in GGGCCC, suggest that a major difference between AnTm and GGGCCC motifs under certain experimental conditions may be in lability and stability of curvature rather than in absolute degree of fixed curvature.

M-PM-D5

CONFORMATIONAL FLEXIBILITY OF NUCLEIC ACIDS: A PICOSECOND ANISOTROPY STUDY USING INTRINSIC FLUORESCENCE. ((Solon Georghiou[1], Joseph M. Beechem[2], Thomas D. Bradrick[1] and Alexander Philippetis[1]))
[1]Molecular Biophysics Lab., Physics Dept., University of Tennessee, Knoxville, TN 37996 and [2]Dept. of Molecular Physiology and Biophysics, Vanderbilt University, Nashville, TN 37232.

The conformational flexibility of the DNA double helix is of great interest because of its potential role in protein recognition, packaging into chromosomes, formation of photodefects, and interaction with drugs. Theory finds that DNA is very flexible; however, there is a scarcity of experimental results which examine intrinsic properties of the DNA bases for the inherent flexibility in solution. We have studied the dynamics of poly(dA)•poly(dT), $(dA)_{20}$•$(dT)_{20}$, and $(dT)_{20}$ in a 50 mM cacodylate, 0.1 M NaCl, pH 7 buffer by using the time-correlated picosecond anisotropy of thymine fluorescence (293 nm excitation/360 nm emission). For all three nucleic acids, large-amplitude fast anisotropy motional modes ranging from tens of picoseconds to a few nanoseconds are observed. These modes are sensitive to sucrose concentration, and are almost completely eliminated at 77% sucrose by volume; this observation strongly supports the motional origin of the observed depolarization of fluorescence. Measurements on the single-stranded $(dT)_{20}$ reveal *slower* overall motions than the double-stranded 20-mer or the polymer ; a similar trend is also observed when using 2-aminopurine (2-AP) as a fluorescent probe in the center of $(dA)_{20}$•$(dT)_{20}$ or $(dT)_{20}$. These observations, taken together, support a mechanism that involves concerted motions in the interior of double-stranded DNA. On the other hand, ethidium bromide used as an extrinsic fluorescent probe in the double-stranded 20-mer and the polymer, reveals much slower motions than those revealed by thymine or 2-AP fluorescence. This work was supported by NIH Research Grant GM38236 (to SG). JMB is an L. P. Markey Scholar.

M-PM-D6

INFLUENCE OF LOOP SEQUENCE AND ADJOINING BASE PAIR IDENTITY ON THE STABILITY OF DNA HAIRPINS. (A.S. Benight, F.J. Gallo, J. Hilario and T.M. Paner) Dept. of Chemistry, Univ. of Illinois, Chicago, IL 60607.

Melting curves were collected in 115 mM Na^+ for the structures formed from the 16 base DNA sequences: 5'-G-G-A-T-A-X-Y-Y-Y-Y-X-T-A-T-C-C-3' and 5'-G-G-A-T-A-X-T-Y-Y-T-X-T-A-T-C-C-3' (X,Y = A,T,G,C). Curves of all 28 molecules were independent of strand concentration over a 60-fold range, indicating these sequences exclusively form intramolecular hairpins. Hairpin stability was found to strongly depend on both loop sequence and identity of the first base pair adjoining the loop. For the hairpins with homogeneous sequence loops, melting temperatures ranged from 33°C for the hairpin with an A_4 loop adjoined by an A·T base pair to 58.3°C for the hairpin with a T_4 loop adjoined by a C·G base pair. Theoretical melting curves were fitted to experimental curves by adjusting the parameters for loop formation. Excellent fits were obtained in all cases and provided empirical evaluation of the dependence of the thermodynamic parameters for loop formation on loop and adjoining base pair sequence. Results indicated deviations from two-state melting behavior for the more stable hairpins due to the greater likelihood of forming loops with at least one broken base pair. Comparisons of the evaluated parameters obtained for the hairpins with homogeneous and heterogeneous sequence loops provided insight into the separate contributions of loop and stem sequence to hairpin stability.

M-PM-D7

^{1}H NMR OF 1, N^2-PROPANO-2'-DEOXYGUANOSINE OPPOSITE A TWO BASE DELETION. ((J.G. Moe, J.P. Weisenseel, G.R. Reddy, L.J. Marnett, and M.P. Stone)) Center in Molecular Toxicology, Departments of Chemistry and Biochemistry, Vanderbilt University, Nashville, TN 37235.

1,N^2-propano-2'-deoxyguanosine (PdG) was inserted into the iterated sequence $(CG)_3$ in an oligonucleotide derived from the *hisD3052* gene of *Salmonella typhimurium*. The modified oligonucleotide was annealed to the complementary strand locating the adduct opposite a two base deletion, which models the slipped intermediate hypothesized to generate two-base deletions at this site.

```
      1          11
5'-ATCGCXCGGCATG-3'        X = PdG
3'-TAGCG··CCGTAC-5'
   22          12
```

^{1}H NMR revealed formation of a stable duplex with a two base bulge localized at X^4C^5. NOEs were observed from PdG to base pairs C^3•G^{18} on the 5' side of the lesion and G^6•C^{17} on the 3' side. PdG was in the *anti* configuration relative to the glycosidic bond; NOE and chemical shift data supported an intrahelical orientation, while the unpaired C^5 was extrahelical. For the modified strand, the sequential NOE connectivities between aromatic and H1' protons were interrupted between X^4 and C^5. Chemical shift perturbations indicated a distortion on the complementary strand at the deoxyribose of C^{17}. Multimeric derivatives of this oligonucleotide migrated anomalously on non-denaturing PAGE indicating induced bending, which was confirmed by structural refinement. Supported by the NIH: CA55678 (M.P.S.), CA47479 (L.J.M.), ES00267 (Toxicology Center), and RR05805 (NMR Spectrometer).

M-PM-D8

THE HYDRATION OF A-, B-, AND Z-DNA STUDIED WITH THE POTENTIALS OF MEAN FORCE APPROACH
((Gerhard Hummer[1], Angel E. García[1], and Dikeos Mario Soumpasis[2]))
[1]Theoretical Biology and Biophysics Group T-10, MS K710, Los Alamos National Laboratory, Los Alamos, NM 87545, U.S.A.; [2]Department of Molecular Biology, Max-Planck-Institute for Biophysical Chemistry, P.O. Box 2841, D-37018 Göttingen, F.R.G. (Sponsored by G. I. Bell)

The hydration of A-, B-, and Z-DNA fiber structures of the sequence $d(CG)_6$ are analysed with the potentials of mean force formalism. The method uses two- and three-particle correlation data of the solvent (*i.e.*, water) combined with positional data of the electronegative atoms on DNA (oxygen and nitrogen) to calculate detailed sequence and structure dependent water density distributions around the molecules. The minor grooves of A-, B-, and Z-DNA are found to contain strongly localized water molecules. However, depending on the local DNA structure and sequence, different patterns emerge. In A-DNA, a banded hydration structure is observed in the minor groove with elongated high water density regions between consecutive base pairs. In B-DNA, the minor groove is occupied by a side-by-side ribbon of high water density; and in Z-DNA, distinct clouds of high water density are found at 5'-C-G steps, whereas 5'-G-C steps show a less pronounced minor groove hydration. In the major groove, water is generally less localized. At 5'-C-G steps of A-DNA, two regions between consecutive bases show comparably high water densities. In Z-DNA, the localization of water at 5'-G-C steps is stronger than at 5'-C-G steps, contrary to the results for the minor groove.

M-PM-D9

DIFFERENTIAL HYDRATION OF dA•dT BASE PAIRS IN PARALLEL DNA RELATIVE TO ANTIPARALLEL DNA
((Dionisios Rentzeperis*, Donald W. Kupke†, and Luis A. Marky*))
*Department of Chemistry, New York University, New York, NY 10003; and †Dept. of Biochemistry, University of Virginia, Charlottesville, VA 22908.

Parallel-stranded DNA is a novel double-stranded helical form of DNA. Its secondary structure is established by *reverse* Watson-Crick base pairing between the bases of the complementary strands forming a double helix with equivalent grooves. We have used a combination of magnetic suspension densimetry and isothermal titration calorimetry to obtain complete thermodynamic profiles for the formation of two DNA 25mer duplexes. The duplexes contain exclusively dA•dT base pairs in either parallel (ps-D1•D2) or antiparallel (aps-D1•D3) orientation. At 15°C, the formation of each duplex is accompanied by favorable free energy terms of -8.2 kcal mol^{-1} (ps-D1•D2) and -9.9 kcal kcal mol^{-1} (aps-D1•D3), exothermic enthalpies and unfavorable entropies, and by an uptake of both counterions and water molecules. If we use the formation of the aps-D1•D3 duplex as a reference state to establish a thermodynamic cycle in which the similar single strands cancel out, we obtained a small $\Delta\Delta G°$ term of +1.7 kcal mol^{-1} that results from a differential enthalpy-entropy compensation of +40.4 kcal mol^{-1}, and a $\Delta\Delta V$ of 257 mL mol^{-1}. The positive sign of this enthalpy-entropy compensation together with the marginal differential counterion uptake of 0.2 mol Na^+ per mol of duplex is characteristic of processes driven by differential hydration and strongly suggest that the parallel duplex is much less hydrated than its antiparallel counterpart by 4 to 5 moles of water per mole of base pair. This work supported by NIH Grants GM-42223 and GM-34938.

M-PM-D10

BIOPHYSICAL PROPERTIES OF SINGLE-STRANDED TRIPLET DNA REPEATS ASSOCIATED WITH TRIPLET REPEAT EXPANSION DISEASES (TREDs). ((M. Mitas, J. Dill, I. S. Haworth, and E. Chambers)) Dept. of Biochemistry and Molecular Biology, Oklahoma State University, 74074. Dept. of Pharmaceutical Sciences, University of Southern California, 90033. (Spon. by M. Nirenberg).

Triplet repeat expansion diseases (TREDs) are unique among the family of inherited genetic disorders. They are characterized by the coincidence of disease manifestation with expansion of a GC-rich trinucleotide repeat contained within the transcribed region of a specific gene. Two fragile X syndromes, Kennedy's disease, Huntington's disease, myotonic dystrophy, and spinocerebellar ataxia type I are members of this family of disease. We report that all of the triplet repeats associated with TREDs are Class I triplet repeat members (p~0.00023), defined by the occurrence of a palindromic GC or CG dinucleotide within the repeat. Since members of Class II triplet repeats (G+C-rich but not containing a palindrome) are virtually identical to Class I repeats at the double-stranded (ds) DNA level, the data suggest that the etiologies of TREDs may reside at the single-stranded (ss) level, possibly due to secondary structures (i.e., hairpins) that form during DNA replication and protein translation. The results of energy minimization, UV absorbance melting, electrophoretic mobility, or ^{31}P-NMR analyses indeed suggest the presence of secondary structures in ss DNA containing triplet repeats of CTG, CAG, CCG, CGG, C^5mCG, and ^{5}mCGG. Electrophoretic mobility studies revealed the following unique features of ss CCG and CGG repeats: 1) $(CCG)_{15}$ and $(C^5mCG)_{15}$ undergo deprotonization at pH 8.1 and 2) Treatment with 8 M urea at 50°c was required for complete removal of secondary structures formed with $(CGG)_{15}$ and $(^5mCGG)_{15}$, whereas treatment with 8 M urea at 20°c was required for the removal of structures formed with the other repeats. These results possibly provide a biophysical basis for triplet repeat expansion associated with Class I triplet repeats, and chromosomal breakage associated with ds CCG triplet repeats.